Multiple Coulomb Excitation of ^{152}Sm, ^{166}Er, and ^{172,174,176}Yb†

R. O. Sayer,* P. H. Stelson, F. K. McGowan, W. T. Milner, and R. L. Robinson

Oak Ridge National Laboratory, Oak Ridge, Tennessee 37830

(Received 22 October 1969)

Multiple Coulomb excitation of the ground-state rotational band of ^{152}Sm, ^{166}Er, and ^{172,174,176}Yb was measured in order to test the predicted ratios of the $B(E2)$ values for a rotational sequence of states. The deexcitation γ rays from the rotational levels were observed in ^{16}O-γ and α-γ conicidence spectra with a Ge(Li) detector. Experimental excitation probabilities are compared to the probabilities calculated with the de Boer–Winther Coulomb-excitation computer program. The $B(E2, 2\rightarrow4)$ and $B(E2, 4\rightarrow6)$ values were determined to accuracies of 6–10%. The $B(E2, 6\rightarrow8)$ values were determined to accuracies of 15–25%. For the poor-rotor ^{152}Sm, the results indicate some increase in the $B(E2)$ values over the rigid-rotor predictions for the higher transitions. The observed increase is less than that predicted by "centrifugal stretching" based on the level positions. However, the results for the four good-rotor nuclei show smaller $B(E2)$ values between higher rotational states than those given by the rigid-rotor values, rather than the larger values predicted by centrifugal stretching.

I. INTRODUCTION

It is well known that the energy spacings of the first few rotational states of even-even rare-earth nuclei are in remarkable agreement with the simple $I(I+1)$ prediction of a rigid rotor. The extent and nature of the small departures from the $I(I+1)$ law, which reflect distortions of the nuclear structure caused by the rotation, are now known in considerable detail from an experimental or phenomenological viewpoint. If one examines this departure by the inclusion of a second term $[E_{(I)}=AI(I+1)-BI^2(I+1)^2]$, one finds $B/A\cong+10^{-3}$ for nuclei in the middle of the rare-earth region, and $B/A\cong+10^{-2}$ for the poorer rotors near the edge of this region.

An interesting question is how best to view these observed distortion effects in terms of the changes in the intrinsic structure of the nucleus. At present, the situation is not clear. Several possible mechanisms have been suggested and investigated theoretically. New types of experimental information on the properties of rotational states have also recently become available.

Centrifugal stretching, i.e., an increase in the moment of inertia caused by an increased deformation β when the nucleus rotates, was suggested as a plausible mechanism for producing the observed departures from the $I(I+1)$ spacings. The experimental work of Stephens *et al.*[1] contributed important new information of the location of higher-spin states of the ground-state band (up to $I=16$) for a number of rare-earth nuclei. Stephens *et al.* tried fitting the observed level spacings both by a series expansion in powers of $I(I+1)$ and by the Davydov-Chaban[2] model. The agreement with the two-parameter Davydov-Chaban model was quite impressive. Diamond *et al.*[3] showed that there is a close connection between the quantum-mechanical Davydov-Chaban model and a classical model of a nucleus undergoing simple centrifugal stretching.

An alternative approach to fitting the level spacings was explored by Harris,[4] who considered the implications of taking the cranking model to higher-order terms in the angular frequency ω. He found that this leads to a moment of inertia that increases with ω, and he was also able to get a very good fit to the experimental data with two free parameters. The Harris result is reminiscent of the Davydov-Chaban theory although no interaction between rotational and vibrational modes is explicitly introduced, and, hence, there is no clear connection between the Harris parameters and those describing a classical stretching.

The moment of inertia of heavy deformed nuclei has been rather successfully calculated by the use of a microscopic model.[5] With this model, it was found that the moment of inertia is quite sensitive to the strength given to the pair correlations. Several theorists[6–8] have suggested that the Coriolis force operating in a rotating nucleus tends to decouple the pairing correlations (reduce the gap) and that this effect could account for the observed energy spacings.

Recent experimental work with muonic x rays and

† Research sponsored by the U.S. Atomic Energy Commission under contract with Union Carbide Corporation.

* Oak Ridge Graduate Fellow from the University of Tennessee under appointment from Oak Ridge Associated Universities. Present address: U.S. Army Nuclear Defense Lab, Edgewood Arsenal, Md.

[1] F. S. Stephens, N. Lark, and R. M. Diamond, Phys. Rev. Letters **12**, 225 (1964).

[2] A. S. Davydov and A. A. Chaban, Nucl. Phys. **20**, 499 (1960).

[3] R. M. Diamond, F. S. Stephens, and W. J. Swiatecki, Phys. Letters **11**, 315 (1964).

[4] S. M. Harris, Phys. Rev. **138**, B509 (1965).

[5] S. G. Nilsson and O. Prior, Kgl. Danske Videnskab. Selskab, Mat.-Fys. Medd. **32**, No. 16 (1961); J. J. Griffin and M. Rich, Phys. Rev. Letters **3**, 342 (1959).

[6] B. R. Mottelson and J. G. Valatin, Phys. Rev. Letters **5**, 511 (1960).

[7] E. R. Marshalek, Phys. Rev. **158**, 993 (1967); Phys. Rev. Letters **20**, 214 (1968).

[8] D. R. Bes, S. Landowne, and M. A. J. Mariscotti, Phys. Rev. **166**, 1045 (1968).

with isomer shifts observed by the Mössbauer effect has provided information on the change in the mean square radius of a rotational nucleus when in the ground state and when in the first 2+ state. The observed change in nuclear size is much less than expected for simple centrifugal stretching.

If rotation increases the distortion of a nucleus, we would expect a departure of the $B(E2)$ values from those predicted for a rigid rotor since these $B(E2)$'s are proportional to β^2. Our present knowledge of $B(E2)$ values within the ground-state rotational band of rare-earth nuclei is much less extensive and also less accurate than the knowledge on level positions. Furthermore, the expected departure of the $B(E2)$ values from those for a rigid rotor, implied by the analysis of level positions in terms of the centrifugal-stretching hypothesis, are not large. For example, a good rotor, such as ^{166}Er, might exhibit a 1% departure from the rigid-rotor prediction for the ratio $B(E2)_{4\to2}/B(E2)_{2\to0}$. The best experimental measurements of this ratio have an accuracy of $\pm7\%$.[9] Thus, the presently available measurements agree well with the rigid-rotor prediction but are not accurate enough to reveal a possible centrifugal-stretching effect. Of course, as one proceeds up the rotational band, the possible departures become larger; for the ratio $B(E2)_{10\to8}/B(E2)_{2\to0}$, one might expect a 10% departure from the rigid-rotor value.

For poor rotors such as ^{152}Sm or ^{154}Gd, the departure of the $E(4+)/E(2+)$ ratio from the rigid-rotor value is such that one might expect centrifugal stretching to produce a 10–15% increase in the ratio $B(E2)_{4\to2}/B(E2)_{2\to0}$. An effect of this size is barely within the reach of experimental techniques. Burde *et al.*[10] have determined the $B(E2)_{4\to2}/B(E2)_{2\to0}$ ratio for ^{154}Gd to be 1.77 ± 0.25, whereas the rigid-rotor value is 1.43, and thus there is some evidence for the existence of the proposed centrifugal-stretching effect for this poor rotor.

Heavy-ion multiple-Coulomb-excitation experiments will yield $B(E2)$ values between higher members of the ground-state rotational band. de Boer *et al.*[11] observed the excitation of states up to the 8+ level for several rare-earth nuclei. The experimental errors for the population of the 4+, 6+, and 8+ states were 8–11%, 15–30%, and 40–60%, respectively. To within these errors, the experimental results agreed with the predictions of the multiple-Coulomb-excitation theory for excitation of a rigid rotor.

In this paper, we report results of multiple-Coulomb-excitation experiments with ^{16}O ions on several even-even rare-earth nuclei.[12] Considerable effort was made to sharpen the experimental accuracy of $B(E2)$ values obtained by this method. The high-resolution Ge(Li) detectors played a very significant role in obtaining increased accuracy. The nuclei ^{172,174,176}Yb and ^{166}Er were chosen because they are among the best rotors in the rare-earth region. To provide a contrasting case, we also studied ^{152}Sm, which is a poor rotor at the edge of the region of strongly deformed nuclei.

II. EXPERIMENTAL METHOD

Multiple Coulomb excitation was produced both by 25- to 52-MeV ^{16}O ions obtained from the ORNL tandem and by 7- to 10-MeV α particles obtained from the 6-MV Van de Graaff.

The targets used in the measurements were metallic foils, ranging in thickness from 20–50 mg/cm^2, made of isotopically enriched material. Isotopic purities exceeded 94% for all five targets. Both Ge(Li) and NaI detectors were used to measure the yield of Coulomb-excited γ rays. Most of the measurements were made with a 5-cc planar Ge(Li) detector. However, toward the end of the work, a 30-cm^3 coaxial Ge(Li) detector was used. The NaI detector was a standard 3-in. diam by 3-in. long crystal mounted on a DuMont 6363 photomultiplier tube.

The determinations of the efficiency of the Ge(Li) γ-ray detector, especially the relative efficiency as a function of the γ-ray energy, are of central importance to the measurements. A set of calibrated γ-ray sources (ranging from a 60-keV ^{241}Am source to a 1836-keV ^{88}Y source) was prepared by measuring the source strengths with a NaI detector of well-known efficiency. These sources were compared later to a set of "Vienna" calibrated γ-ray sources that had γ-ray source strengths determined to accuracies of 2% or better.[13] The two sets of sources were found to be in reasonable agreement. We therefore believe that the relative efficiency was known to $\pm2\%$ for γ rays of not too different energy and was known to $\pm5\%$ for γ rays of widely differing energies.

Thick-target γ-ray yields were measured with the target inclined 45° with respect to the incident beam. The yields were measured with the detector at 235° to minimize absorption by the target material.

Much of the experimental work involved coincidence measurements between the γ rays and exciting projectiles backscattered into an annular-silicon surface-barrier detector. The annular-particle detector subtended the angular range 151°–169° in the laboratory system for one set of measurements and subtended the angular range 157°–171° for another set of measurements. Since thick targets were used in these experiments, the actual target thickness for the Coulomb-excitation measurements was determined by the energy

[9] H. W. Kugel, E. G. Funk, and J. W. Mihelich, Phys. Rev. **165**, 1352 (1968).
[10] J. Burde, M. Rakavy, and G. Rakavy, Phys. Rev. **129**, 2147 (1963).
[11] J. de Boer, G. Goldring, and H. Winkler, Phys. Rev. **134**, B1032 (1964).
[12] See also R. O. Sayer, P. H. Stelson, F. K. McGowan, W. T. Milner, and R. L. Robinson, Bull. Am. Phys. Soc. **12**, 1201 (1967).
[13] Sources made by Division of Research and Laboratories, International Atomic Energy Agency, Vienna, Austria.

TABLE I. Summary of states observed to be Coulomb-excited in the five nuclei ^{152}Sm, ^{166}Er, and ^{172,174,176}Yb. In column 4, we list the γ rays observed, and these are attributed to the excitation of levels given in column 2. The last column lists the values for the total internal-conversion coefficient α_T, which we have used for the γ-ray transitions given in column 4.

Nucleus	Level (keV)	J^π	E_γ (keV)	J_f	α_T
^{152}Sm	121.78[a]	2+	121.78[a]	0	1.18
	366.5±0.3	4+	244.7±0.3	2	0.109
	684.6±0.3	0+	562.8±0.3	2	0.010
	707.2±0.4	6+	340.7±0.3	4	0.039
	810.6±0.3	2+	443.9±0.3	4	0.018
			689.0±0.3	2	0.008
			810.4±0.5	0	0.004
	1042.6±0.7	3−	675.8±0.7	4	0.002
			920.8±0.7	2	0.001
	1086.0±0.3	2+	964.2±0.3	2	0.004
			1086.0±0.3	0	0.002
^{166}Er	80.57[b]	2+	80.57[b]	0	6.88
	265.0±0.3	4+	184.4±0.3	2	0.336
	545.5±0.5	6+	280.5±0.4	4	0.086
	786.1±0.3	2+	705.4±0.4	2	0.007
			786.2±0.4	0	0.006
^{172}Yb	78.70[b]	2+	78.70[b]	0	8.40
	260.3	4+	181.59[c]	2	0.380
	540.0±0.3	6+	279.7±0.3	4	0.093
	911.5±3.0	8+	371.5±3.0	6	0.041
	1117.2±0.5	2+	856.4±0.5	4	0.005
			1038.8±0.6	2	0.003
			1117.4±1.0	0	0.003
	1466.5±0.4	2+	1387.8±0.4	2	0.002
			1466.6±0.6	0	0.002
	1609.7±0.8	2+	1530.3±1.0	2	0.002
			1610.5±1.0	0	0.002
^{174}Yb	76.46[b]	2+	76.46[b]	0	9.35
	253.1±0.3	4+	176.6±0.3	2	0.420
	526.0±0.5	6+	272.9±0.4	4	0.100
	892.0±4.0	8+	366.0±4.0	6	0.042
^{176}Yb	82.13[b]	2+	82.13[b]	0	7.08
	271.69±0.25	4+	189.56±0.25	2	0.325
	564.8±0.4	6+	293.1±0.3	4	0.081
	955.1±0.9	8+	390.3±0.8	6	0.035
	1261.2±0.4	2+	1178.9±0.4	2	0.002
			1261.4±0.5	0	0.002

[a] I. Marklund and B. Lindstrom, Nucl. Phys. **40**, 329 (1963).
[b] E. L. Chupp, W. M. DuMond, F. J. Gordan, R. C. Jopson, and H. Mark, Phys. Rev. **112**, 518 (1958).
[c] V. V. Tuchkevich, V. A. Romanov, and M. G. Totubalina, Izv. Akad. Nauk. SSSR, Ser. Fiz. **27**, 246 (1963) [English transl.: Bull. Acad. Sci. USSR, Phys. Ser. **27**, 258 (1963)].

cutoff in the annular detector. It was therefore importnat to accurately determine the energy response of the annular detector for both α particles and ^{16}O ions. This was done both by variation of the beam energy incident on the target and (in the case of ^{16}O) by using targets of different atomic weight. Typical target thicknesses for ^{16}O ions were 8–11 MeV.

Particle γ-ray coincidences were measured with the γ-ray detector located at several different angles with respect to the incident beam.

III. EXPERIMENTAL RESULTS

The experimental results are for thick-target γ-ray yields and backscattered-particles–γ-ray coincidence yields for both α-particle and ^{16}O ion projectiles. The extraction of $B(E2)$ values from γ-ray yield information requires the knowledge of total internal conversion coefficients α_T. The values we have used together with a summary of the states observed to be Coulomb-excited are given in Table I. (The higher 2+ levels will be

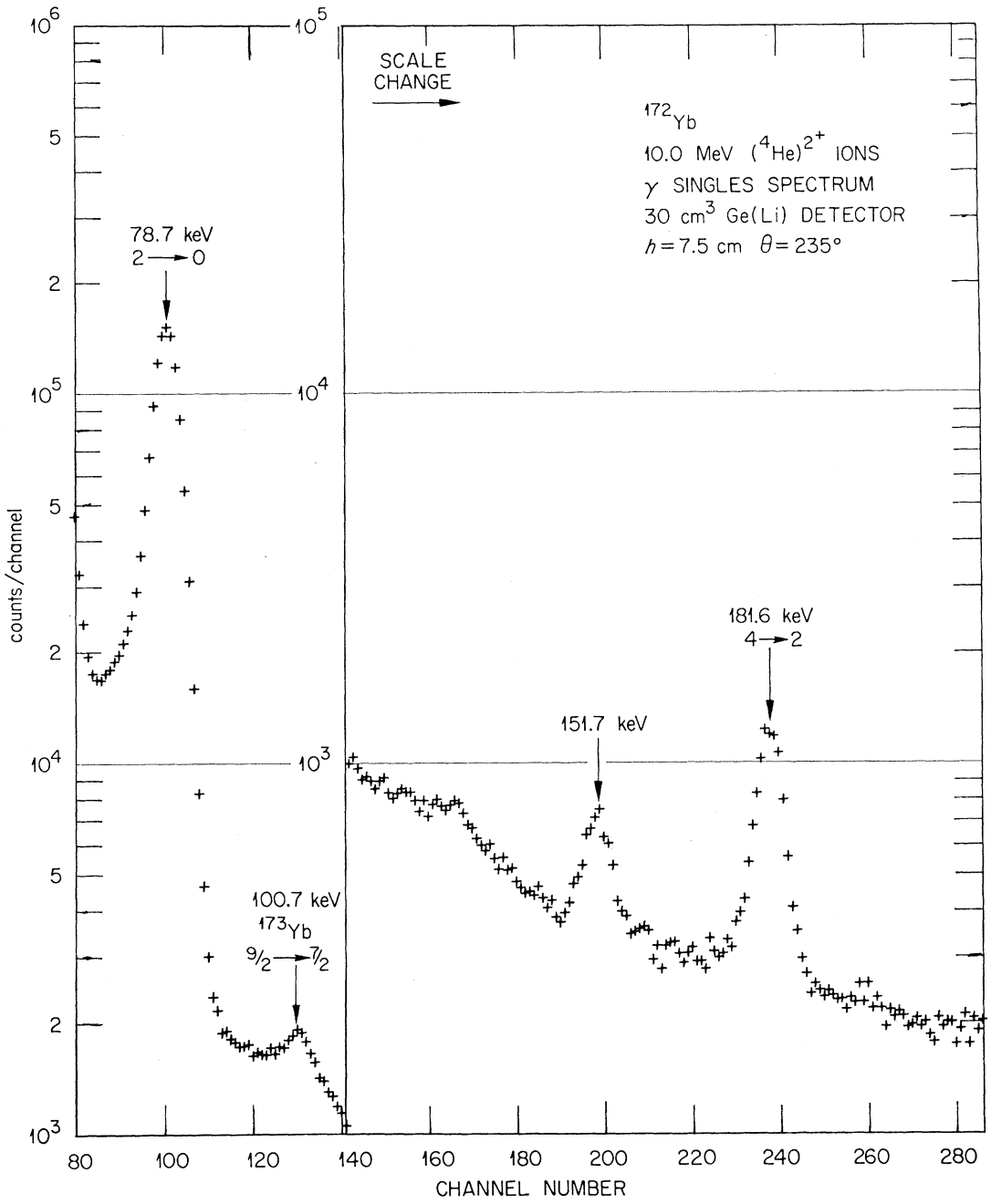

FIG. 1. A Ge(Li)-detector pulse-height spectrum of the γ rays resulting from the Coulomb excitation of a ^{172}Yb target by ^{4}He ions.

discussed in a forthcoming publication.) We have assigned an error of ±4% to values taken for the α_T values. The α_T values were obtained from the tables of Sliv and Band[14] by use of the prescription $\alpha_T = \alpha_K + 1.33\alpha_L$. For some of the 2→0 transitions where α_T is quite large, we checked the Sliv and Band α_K and α_L values with the more recent theoretical calculations of Hager and Seltzer.[15] The two sets of values agree to within 1%.

The 8+ level and the three higher 2+ levels in ^{172}Yb had not been previously observed by Coulomb excitation, although the 1466.5- and 1609.7-keV levels were established from the decay of ^{172}Tm. The existence of the

[14] L. A. Sliv and I. M. Band, *Internal Conversion Coefficients* (North-Holland Publishing Co., Amsterdam, 1958).

[15] R. S. Hager and E. C. Seltzer, Nucl. Data **A4**, 1 (1968).

TABLE II. Summary of γ-ray-yield measurements and $B(E2)$ values for the first 2+ and 4+ states resulting from ^{4}He Coulomb excitation. The quantities $Y_{0\to2}$ and $Y_{0\to2\to4}$ are defined by Eq. (1) of the text. The quantities I_{E2} and I_{E2E2} are defined by Eqs. (3) and (4) of the text.

Nucleus	E_{2+} (keV)	E_{4+} (keV)	^{4}He ion energy (MeV)	$Y_{0\to2}$ (10^7 exc/μC)	I_{E2}[a] (MeV mg/cm^2)	$B(E2;0\to2)$ (e^2 10^{-48} cm^4)	$Y_{0\to2\to4}$ (10^4 exc/μC)	$I_{E2E2}(4)$ (MeV^4 mg/cm^2)	$B(E2;2\to4)$ (e^2 10^{-48} cm^4)
^{152}Sm	121.8	366.5	7.00	1.035	51.0	3.43	...	...	...
			8.00	1.556	78.2	3.36	0.667	319.	1.91
			9.00	2.315	111.8	3.50	1.609	705.	1.97
			10.00	3.154	151.9	3.51	3.271	1388.	2.00
^{172}Yb	78.7	260.3	7.00	1.532	63.5	5.95	0.525	175.	3.55
			8.00	2.227	93.0	5.90	1.158	426.	3.24
			9.00	3.113	128.4	5.98	2.471	899.	3.24
			10.00	4.104	169.8	5.96	4.511	1720.	3.10
^{174}Yb	76.5	253.1	7.00	1.508	63.9	5.81	0.456	179.	3.07
			8.00	2.210	93.3	5.83	1.078	433.	3.00
			9.00	3.099	128.6	5.94	2.370	912.	3.07
			10.00	4.112	169.7	5.97	4.387	1739.	2.97
^{176}Yb	82.1	271.7	7.00	1.367	62.8	5.36	0.356	168.	2.77
			8.00	1.984	92.4	5.29	0.894	413.	2.89
			9.00	2.777	128.0	5.34	1.984	879.	2.96
			10.00	3.735	169.7	5.42	3.625	1690.	2.78

[a] Corrected for absorption of the γ rays by the target.

1117.2-keV level in ^{172}Yb is still somewhat uncertain. de Boer *et al.*[11] interpreted a 345-keV γ ray in one of their Coulomb-excitation spectra as the 8→6 γ ray from ^{174}Yb. From this work and the radioactive decay studies, however, this γ-ray energy is (366±4) keV. Thus, de Boer *et al.* probably observed the (2→0)+(6→4) coincidence-sum peak that would appear at 349 keV. All other levels given in Table I have been established from previous Coulomb excitation and from radioactive-decay studies.

A. Thick-Target Coulomb Excitation of the 4+ State with α-Particle Projectiles

Multiple-Coulomb-excitation probabilities are quite small for α particles, and, therefore, second-order perturbation theory should provide an accurate description of the process. We have observed the thick-target γ-ray yields for excitation of the 2+ and 4+ rotational states in ^{152}Sm and ^{172,174,176}Yb by 7–10-MeV α particles. The $B(E2)_{4\to2}$ values are extracted by the use of the double-$E2$ perturbation theory.

A representative γ-ray spectrum, resulting from bombardment of ^{172}Yb with 10-MeV α particles, is shown in Fig. 1. The relative intensity of the 2→0 and 4→2 γ rays is about 120. Recalling, however, that $\alpha_T=8.40$ for the 2→0 γ ray, we see that there is roughly one excitation of the 4+ state per 1000 excitations of the 2+ state.

The 100.7-keV peak in Fig. 1 is assigned to the $\frac{9}{2}\to\frac{7}{2}$ transition in the impurity isotope ^{173}Yb. The expected $\frac{9}{2}\to\frac{5}{2}$ transition in ^{173}Yb produces a γ ray of 179.5 keV and can not be resolved from the 181.6-keV 4+→2+ γ ray of interest. We can, however, accurately estimate the intensity of this γ ray and subtract its yield. It contributes 12–19% of the observed yield for ^{172}Yb and 6–15% for ^{174}Yb. For ^{176}Yb, the two peaks were separated by 10 keV and were easily resolved.

Table II presents the experimental yields and $B(E2)$ values. The thick-target Coulomb-excitation yield Y, measured in units of excitations per microcoulomb (exc/μC) of incident charge, is given by the formula

$$Y(\text{exc}/\mu\text{C})=(q\mathfrak{A})^{-1}[(1+\alpha_T)N/\bar{W}T_\gamma\epsilon-T_c], \quad (1)$$

where q is the charge in microcoulombs collected during the run, $\mathfrak{A}$ is the fractional isotopic abundance, α_T is the total conversion coefficient, N is the counts in the full-energy γ-ray peak, and ϵ is the γ-ray detector efficiency. T_γ is the transmission coefficient that accounts for the absorption of γ rays by the target material. $\bar{W}$ is the factor that corrects for the anisotropic γ-ray angular distribution. Finally, the quantity T_c is the number of transitions from the state of interest that are due to cascade transitions from higher-lying states to the state of interest.

The $B(E2)$ for excitation of the first 2+ state is given by the formula

$$B(E2;0\to2)=\frac{5.554\times10^{-59}zA_2'(CZ_2)^2Y(\text{exc}/\mu\text{C})}{A_1I_{E2}}\ e^2\text{cm}^4, \quad (2)$$

TABLE III. Summary of $B(E2)$ values obtained from γ-ray yields with ^{4}He Coulomb excitation.

Nucleus	$B(E2;0\to2)_{\text{expt}}$	$B(E2;0\to2)$[a]	$B(E2;2\to4)_{\text{expt}}$	$B(E2;4\to2)$[b] / $B(E2;2\to0)$
	$B(E2)$ values in units of $e^2\,10^{-48}$ cm^4			
^{152}Sm	3.45±0.28	3.40±0.12	1.98±0.16	1.62±0.13
^{172}Yb	5.95±0.48	6.00±0.12	3.24±0.23	1.50±0.11
^{174}Yb	5.89±0.47	5.70±0.20	3.03±0.21	1.48±0.11
^{176}Yb	5.35±0.43	5.45±0.35	2.85±0.20	1.45±0.14
			Symmetric rotator	1.429

[a] From P. H. Stelson and L. Grodzins, Ref. 18.

[b] Computed from the values in columns 3 and 4.

where

$$I_{E2}=\int_0^{E_i}\frac{(E-C\Delta E)f_{E2}(\eta_i,\xi)}{S(E)}\,dE\,\frac{\text{MeV}}{\text{mg/cm}^2}. \quad (3)$$

Here, z is the projectile charge state, Y is the thick-target yield in excitations per microcoulomb, A_2' is the target atomic weight (normal element), A_1 and A_2 are the masses of projectile and target in amu, Z_2 is the target nuclear charge, E_i is the incident projectile energy in MeV, ΔE is the nuclear-excitation energy in MeV, and $C=1+A_1/A_2$. The projectile stopping power, $S(E)\equiv dE/d\rho\,x$ is measured in units of MeV cm^2/mg. The integral I_{E2} was evaluated numerically for each case of interest using the $f_{E2}(\xi)$ values tabulated by Alder *et al.*[16]

The total cross section for double-$E2$ Coulomb excitation of a 4+ state is proportional to the product $B(E2)_{0\to2}\times B(E2)_{2\to4}$. This product, then, is proportional to the 4+ yield $Y_{0\to2\to4}$ and inversely proportional to a thick-target integral defined by

$$I_{E2E2}(4+)=\int_0^{E_i}\frac{\beta(E)F(\xi_1,\xi_2)}{S(E)}\,dE\,\frac{\text{MeV}^4}{\text{mg/cm}^2}, \quad (4)$$

where $\beta(E)=E^2(E-C\Delta E_1)(E-C\Delta E_1-C\Delta E_2)$. Here, ΔE_1 is the excitation energy of the 2+ state (MeV) and $\Delta E_1+\Delta E_2$ is the excitation energy of the 4+ state in MeV. The functions $F(\xi_1,\xi_2)$ are defined and tabulated by Douglas.[17] Comparison of the expressions for the 2+ and 4+ yields gives the formula

$$B(E2;2\to4)=1.084\times10^{-51}$$
$$\times[Z_1^2(CZ_2)^4/A_1](Y_{0\to2\to4}I_{E2}/Y_{0\to2}I_{E2E2})\,e^2\text{ cm}^4. \quad (5)$$

This formula indicates some useful cancellations that are in effect when we make a simultaneous measurement of the Coulomb-excitation yields for the 2+ and 4+ states. Only the relative γ-ray efficiency enters, and, to a large extent, the stopping power cancels out. The stopping powers used to calculate the I_{E2} and I_{E2E2} values listed in Table II were as follows: For the Yb targets $S(E)=0.541\,E^{-0.481}$ MeV cm^2/mg and for the ^{152}Sm target $S(E)=0.596\,E^{-0.480}$ MeV cm^2/mg. We think these stopping powers are accurate to ±4%.

An inspection of the values for $B(E2)_{0\to2}$ and $B(E2)_{2\to4}$ shows that they are constant within the relative errors of 1% for $B(E2)_{0\to2}$ and 2–4% for $B(E2)_{2\to4}$. Table III summarizes these measurements and compares the ratio $B(E2)_{4\to2}/B(E2)_{2\to0}$ with the rigid-rotor value. The values given in Table III are the weighted averages of the values of Table II. Absolute errors are quoted. The more accurate $B(E2)_{0\to2}$ values compiled by Stelson and Grodzins[18] were used to compute the ratio

TABLE IV. Comparison of experimental and theoretical Coulomb excitation of the 2+ and 4+ rotational states in ^{176}Yb by ^{16}O ions with energies of 25–42 MeV. The theoretical values are based on the use of the Winther–de Boer computer program for Coulomb excitation.

Nucleus	$B(E2;0\to2)$ (e^2 10^{-48} cm^4)	^{16}O ion energy (MeV)	2+ Yield Experiment (10^7 exc/μC)	2+ Yield Theory[a] (10^7 exc/μC)	2+ Yield Experiment/Theory	4+ Yield Experiment (10^5 exc/μC)	4+ Yield Theory[a] (10^5 exc/μC)	4+ Yield Experiment/Theory
^{176}Yb	5.61[b]	25.0	1.930	1.834	1.052	0.363	0.359	1.011±0.007
		30.0	3.183	3.038	1.048	1.223	1.207	1.013±0.007
		36.0	5.097	4.840	1.053	3.793	3.673	1.033±0.008
		42.0	7.291	7.014	1.039	9.121	8.899	1.025±0.009

[a] Theoretical yields were calculated with the modified Winther–de Boer computer program using the rotational-model matrix elements:

$$\langle J_i\,||\,i^2M(E2)\,||\,J_f\rangle=-(-1)^{J_i-J_f}(2J_i+1)^{1/2}\,C(J_i2J_f;00)\,[B(E2;0\to2)]^{1/2}.$$

[16] K. Alder, A. Bohr, T. Huus, B. R. Mottelson, and A. Winther, Rev. Mod. Phys. **28**, 432 (1956).
[17] A. C. Douglas, AWRE Report No. NP/*P*-2/62, 1962 (unpublished).
[18] P. H. Stelson and L. Grodzins, Nucl. Data **1**, 21 (1965).

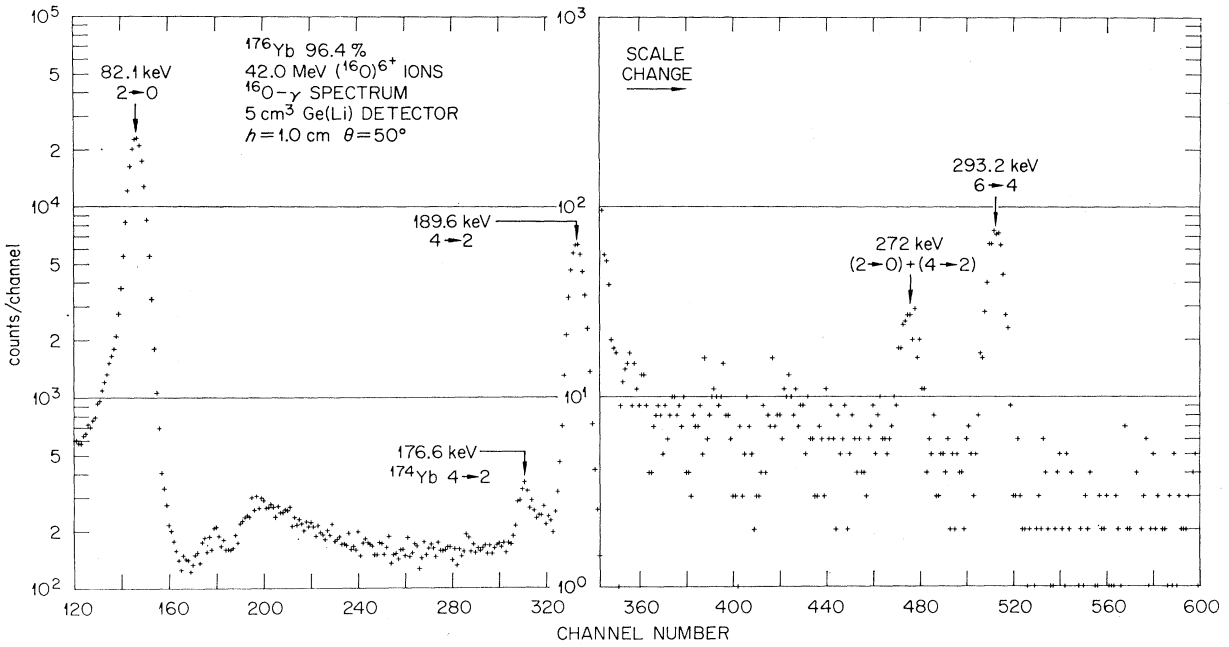

FIG. 2. Ge(Li)-detector pulse-height spectrum of the γ rays in coincidence with ^{16}O ions backscattered from a ^{176}Yb target.

$B(E2)_{4\to2}/B(E2)_{2\to0}$. The excellent agreement (1–3%) of the present $B(E2)_{0\to2}$ values with the previous more accurate values is fortuitous. The error in the relative $B(E2)_{0\to2}$ values for Yb isotopes, however, is less than 3% if we assume that the relative error in α_T is $\pm2\%$.

The observed double-$E2$ excitation of the 4+ states with α particles is in excellent agreement with the predictions of second-order perturbation theory. The values obtained for $B(E2)_{4\to2}$ have an accuracy as good as, but not much better than, the best values obtained from lifetime measurements.

B. Thick Target Coulomb Excitation of the 4+ States with ^{16}O

Thick-target γ-ray yield measurements were made for the Coulomb excitation of the 2+ and 4+ states produced by incident ^{16}O ions of 25–45.5 MeV for the three different Yb targets. To illustrate these results, the experimental yields of the 2+ and 4+ states for ^{176}Yb are given in Table IV. The second-order perturbation theory is not adequate for the interpretation of these experiments because the excitation probabilities are too large. If one uses the perturbation interpretation, the $B(E2)_{0\to2}$ and $B(E2)_{2\to4}$ values systematically decrease by about 8% as one proceeds from 25- to 42-MeV excitation energy.

TABLE V. Values used for the stopping power of ^{16}O ions in ytterbium.

$E(^{16}O)$ (MeV)	$S(E)$ MeV(cm²/mg)
55	2.02
50	2.10
45	2.18
40	2.27
35	2.35
30	2.43
25	2.51
20	2.60
15	2.70
10	2.72
5	2.44

Recently, Winther and de Boer developed a computer program to evaluate the excitation amplitudes for multiple-$E2$ Coulomb excitation by direct numerical integration of the coupled differential equations.[19] Input data consist of the nuclear charges and masses, spin and energies of all the nuclear levels under consideration, projectile energy and scattering angle, and all $E2$ reduced-matrix elements. The program then computes excitation probabilities, differential cross sections, and angular distributions of the deexcitation γ rays. The Winther–de Boer program is independent of any specific nuclear model.

We have augmented the Winther–de Boer program to provide integrated results over angle and energy. A detailed description of this program, called MCEX, is available. The calculated results of the program are given in Table IV under the columns labeled theory. For ^{176}Yb, we used the $B(E2;0\to2)$ given by Stelson and Grodzins (5.45×10^{-48} e^2 cm^4) and used the rigid-rotor value of $B(E2)_{2\to4}$ to calculate the yield of the 4+ state The calculated integrals also require the input of $S(E)$

[19] K. Alder and A. Winther, in *Coulomb Excitation* (Academic Press Inc., New York, 1966).

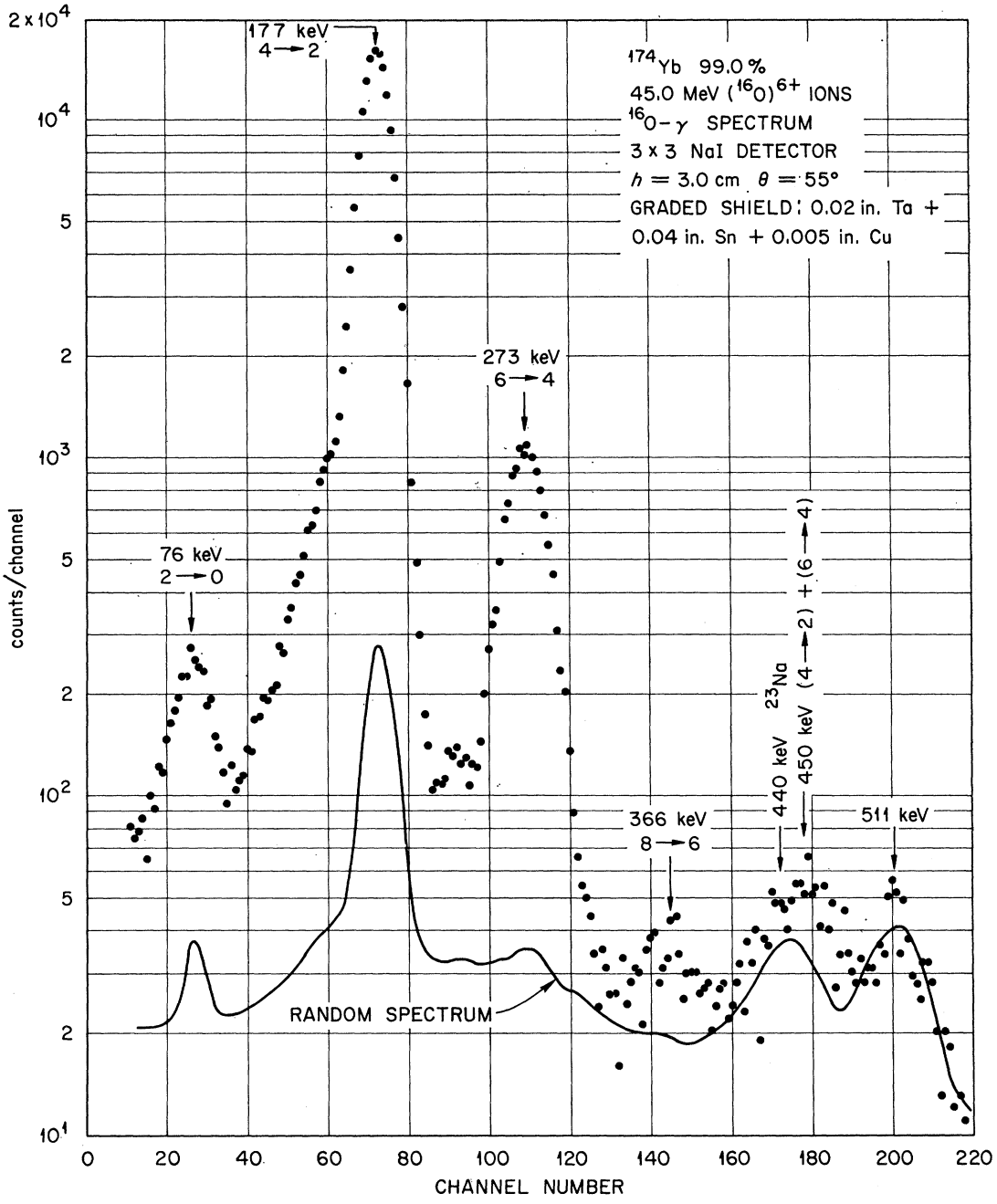

FIG. 3. NaI-scintillation-detector pulse-height spectrum of the γ rays in coincidence with ^{16}O ions backscattered from a ^{174}Yb target.

for ^{16}O ions. Table V gives the values we have used for $S(E)$ for the Yb targets.

For the range of ^{16}O-ion energy used. the excitations per μC for the 4+ state changed by a factor of 20. Yet the ratio of experimental excitations to calculated excitations (last column of Table IV) remains constant to within the errors of approximately 1%. A similar conclusion holds for the 2+ state.

C. Coulomb-Excitation Particle γ-Ray Coincidence Measurements

In order to study the excitation of higher-rotational states by multiple Coulomb excitation, it is advantageous to observe the γ rays in coincidence with backscattered projectiles because these events represent the close collisions that favor the multiple-excitation

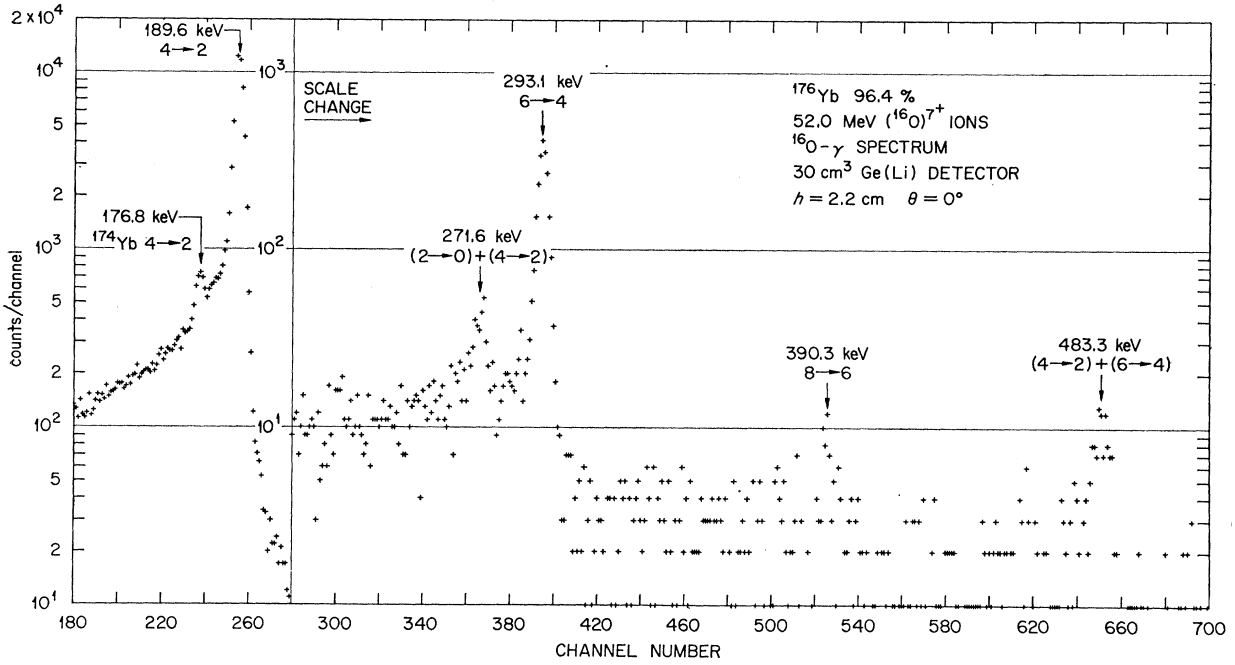

FIG. 4. Ge(Li)-detector pulse-height spectrum of the γ rays in coincidence with ^{16}O ions backscattered from a ^{176}Yb target.

process. Examples of such coincidence spectra are shown in Figs. 2, 3, and 4. In Fig. 2, we show the results for 42-MeV ^{16}O ions on ^{176}Yb and for the 5-cm^3 Ge(Li) detector. The γ ray from the $6+\rightarrow 4+$ transition is clearly seen. Figure 3 is an example of a coincidence spectrum taken with a NaI detector. The γ ray from the $8+\rightarrow 6+$ transition in ^{174}Yb is seen, but only rather weakly. Finally, Fig. 4 shows a coincidence spectrum obtained with a 30-cm^3 Ge(Li) detector. The γ ray from the $8+\rightarrow 6+$ transition in ^{176}Yb is definitely seen, but the total number of counts in the peak is small.

The experimental Coulomb-excitation probability $(P_J)_{\text{expt}}$ is defined as the number of observed excitations of the state J divided by $N_B(E_{\text{cut}})$, the number of particles that scatter into the solid angle of the annular detector and produce pulses large enough to be passed by the lower-level discriminator, which in turn defines the target thickness. The number of Coulomb excitations of state J is deduced from the observed number of deexcitation γ rays from state J to state $J-2$ since this is the only significant mode of decay for the states in the ground-state rotational band. A correction, however, must be applied to take into account the subsequent feeding of a given state J by the γ-ray decay to this state from the decay of higher-rotational states. Another conceivable correction results from Coulomb excitation of high-lying 2+ states which then decay to the different states of the ground-state rotational band. For the present cases, we find that the intensities of such feedings are so small that they can safely be neglected.

The expression for $(P_J)_{\text{expt}}$ is analogous to that given by formula (1) with q replaced by $N_B(E_{\text{cut}})$ and with the understanding that the quantities N, α, $\bar{W}$, T_γ, and ϵ_γ all refer to the γ-ray transition $J\rightarrow J-2$. The quantity T_c is the correction for the feeding from the higher states of the rotational band;

$$T_c=[(1+\alpha_{J+2})N_{J+2}]/[\bar{W}_{J+2}(T_\gamma)_{J+2}\epsilon_{J+2}]. \quad (6)$$

A summary of the experimental results is given in Table VI. Columns 2 and 3 give the incident ^{16}O energy and the minimum ^{16}O energy (for elastic scattering). Columns 4–7 list the $(P_J)_{\text{expt}}$ for the 2, 4, 6, and 8 states, respectively.

We now want to compare the experimental $(P_J)_{\text{expt}}$ values to those expected theoretically for a rigid rotor. We have

$$(P_J)_{\text{theor}}=\left(\int_{E_i}^{E_{\text{cut}}(J)}\frac{dE}{S(E)}\int d\Omega_L\frac{d\sigma_J(\theta_L,E)}{d\Omega_L}\right)\Big/\left(\int_{E_i}^{E_{\text{cut}}(0)}\frac{dE}{S(E)}\int d\Omega_L\frac{d\sigma_R(\theta_L,E)}{d\Omega_L}\right). \quad (7)$$

The Winther–de Boer program was used to calculate $d\sigma_J(\theta_{CM},E)/d\Omega_{CM}$, and this was then related to the laboratory differential cross section. The $d\theta_R(\theta_L,E)/d\Omega_L$ is the Rutherford cross section. The rotational-model matrix elements for the Winther–de Boer program are

$$\langle J_i\,||\,i^2M(E2)\,||\,J_f\rangle=-(-1)^{J_i-J_f}(2J_i+1)^{1/2}C(J_i2J_f;00)[B(E2,0\rightarrow 2)]^{1/2}. \quad (8)$$

TABLE VI. Coulomb-excitation probabilities of rotational states obtained from ^{16}O-γ coincidence measurements. The quantity P_J is defined by Eq. (7) in the text. The quantity $R(J/J-2) \equiv P_J/P_{J-2}$. The last column of the Table contains the ratio of the quantities in column 11 to those in column 10. $R(J/I) = P_J/P_I$. Errors given in columns 10 and 11 do not include uncertainties in the $B(E2; 0 \rightarrow 2)$ values.

Nucleus	E_i (MeV)	$E_{cut}(0)$ (MeV)	$10^1 P_2$	$10^2 P_4$	$10^4 P_6$	$10^5 P_8$	$10^2 R(6/4)$	$10^2 R(8/6)$	$\frac{R(6/4)_{expt}}{R(6/4)_{theor}}$	$\frac{R(8/6)_{expt}}{R(8/6)_{theor}}$	Expt/Theor $\frac{R(8/6)}{R(6/4)}$
^{152}Sm	42.00	32.62	3.20	1.74	4.10	...	2.35	...	1.072±0.107	...	...
^{166}Er	42.00	34.82	3.49	3.41	9.23	...	2.71	...	0.865±0.049	...	...
^{172}Yb	45.10	36.47	4.72	4.25	14.68	...	3.46	...	0.963±0.100	...	...
	45.50	35.97	2.86[a]	2.73[a]	9.95[a]	...	3.64	...	0.986±0.111	...	...
	52.00	42.67	2.26[a]	3.63[a]	2.32[a]	...	6.40	...	1.007±0.105	...	...
	45.50	35.67	...	4.03	13.59	...	3.37	...	0.909±0.066	...	...
	45.50	35.34	...	3.97	13.21	1.75	3.31	1.32	0.932±0.061	0.77±0.19	0.82±0.21
	45.00	35.31	3.29	3.83	12.98	...	3.39	...	0.958±0.063	...	...
^{174}Yb	45.10	36.47	4.58	4.08	12.32	...	3.02	...	0.847±0.093	...	...
	45.00	35.35	2.83	3.59	12.10	...	3.37	...	0.960±0.068	...	...
	45.00	38.42	...	3.89	14.94	2.24	3.84	1.50	1.015±0.079	0.86±0.21	0.85±0.21
^{176}Yb	42.00	34.57	3.35	2.62	5.94	...	2.26	...	0.898±0.057	...	...
	52.00	40.92	...	7.58	39.32	9.89	5.19	2.52	0.943±0.054	0.92±0.18	0.98±0.20
	52.00	40.52	...	7.58[a]	35.85[a]	7.36[a]	4.73	2.05	0.868±0.046	0.76±0.18	0.87±0.20

[a] Relative values.

TABLE VII. Summary of the $B(E2, 4\rightarrow6)$ and $B(E2, 6\rightarrow8)$ values extracted from the ^{16}O-γ coincidence measurements. The $B(E2, 0\rightarrow2)$ were taken from Ref. 18, and the error in this quantity is included in the quoted errors of the ratio of $B(E2)$ values given in the last three columns.

Nucleus	$B(E2;4\rightarrow6)$ ($e^2\,10^{-48}$ cm^4)	$B(E2;6\rightarrow8)$ ($e^2\,10^{-48}$ cm^4)	$\frac{B(E2;6\rightarrow4)}{B(E2;2\rightarrow0)}$	$\frac{B(E2;8\rightarrow6)}{B(E2;2\rightarrow0)}$	$\frac{B(E2;8\rightarrow6)}{B(E2;6\rightarrow4)}$
^{152}Sm	1.66±0.17	...	1.68±0.18	...	...
^{166}Er	2.27±0.13	...	1.36±0.09	...	...
^{172}Yb	2.54±0.13	1.94±0.49	1.46±0.09	1.24±0.32	0.86±0.22
^{174}Yb	2.51±0.14	2.14±0.52	1.53±0.10	1.43±0.35	0.89±0.22
^{176}Yb	2.23±0.10	2.00±0.31	1.41±0.11	1.40±0.23	0.97±0.15
		Symmetric rotator	1.573	1.647	1.047

Thus, the theoretical P_J values depend on the value taken for $B(E2, 0\rightarrow2)$. In fact, any uncertainty in the value for $B(E2, 0\rightarrow2)$ is amplified in the predicted values for P_J as one goes up the rotational sequence. For example, a 3% change in $B(E2, 0\rightarrow2)$ results in a 12% change in P_8. It is preferable, for this reason, to consider the ratio $R(J/J-2)\equiv P_J/P_{J-2}$. This ratio depends primarily on the $B(E2, J-2\rightarrow J)$, and, hence, the ratios $R(6/4)$ and $R(8/6)$ provide more sensitive tests of the rotational model. In calculating the P_J values, we have used the $B(E2, 0\rightarrow2)$ values given by Stelson and Grodzins. Columns 10 and 11 give the ratios $R(6/4)_{\text{expt}}/R(6/4)_{\text{theor}}$ and $R(8/6)_{\text{expt}}/R(8/6)_{\text{theor}}$, respectively. In Table VI, the errors given reflect only our experimental errors and do not include the uncertainties in the $B(E2, 0\rightarrow2)$. The last column of Table VI gives the ratio of expt/theor for the quantity $R(8/6)/R(6/4)$.

The theoretical P_J values also depend on the values assigned to the static-quadrupole moments Q_J of the rotational states. We have used the rigid-rotor values (prolate shape) for the Q_J values. The theoretical P_J values, however, are not strongly dependent on the values taken for the Q_J. For example, setting Q_6 equal to zero rather than to the rotational value only increases P_6 by 10%. Thus, a 20% deviation in Q_6 from the rigid-rotor value only changes $R(6/4)_{\text{theor}}$ by 2%, which is small compared to the uncertainty in $R(6/4)_{\text{expt}}$.

In principle, the theoretical P_J values are influenced by interference terms originating from the virtual Coulomb excitation of higher 2+ states. The magnitude of these interference terms is calculable if we know the relevant $B(E2)$'s, but we do not know the sign of the interference terms. We have used the Winther–de Boer program to theoretically estimate the size of the interference effects in several cases where there seemed a chance that they might be significant.

Case 1. The influence of the 2+ β-vibrational state at 811 keV in ^{152}Sm on the P_4. Coulomb excitation was by α particles in the energy range 13–9.7 MeV scattered at $\theta=163°$. The inclusion of the 811-keV state changed P_4 by $\pm1.2\%$, depending on the signs taken for the matrix elements.

Case 2. The influence of the 2+ γ-vibrational state at 786 keV in ^{166}Er on the P_4. Coulomb excitation was by α particles in the energy range 14–10.3 MeV, scattered at $\theta=158°$. The inclusion of the 786-keV state changed P_4 by $\pm1.2\%$, depending on the signs taken for the matrix elements.

Case 3. The same as case 2 but with ^{16}O projectiles in the energy range 40–31 MeV, scattered at $\theta=158°$. The inclusion of the 786-keV state changed P_4 by $\pm1\%$.

In all three cases considered, the changes in P_4 are considerably smaller than our present experimental accuracy, and we therefore ignored these interference effects. However, it should be realized that for a good rotor, such as ^{166}Er, the size of the interference effects are comparable to the changes in P_4 predicted by centrifugal stretching.

We also need to consider the influence on P_4 caused by an $E4$ excitation of the 4+ state. Hendrie *et al.*[20] made optical-model analyses of their experimental work on the scattering of α particles by rare-earth nuclei. They found evidence for β_4 deformations in these nuclei. The results suggest that β_4 is +0.05 at the beginning of the rare earths, then decreases to zero at erbium and continues to negative values of −0.07 at the upper end of the rare earths. These β_4 values imply $B(E4, 0\rightarrow4)$ values as large as 5–10 single-particle units.

For 11-MeV α particles on ^{152}Sm, we calculate that the differential cross sections at 160° are in the ratio 100:1 for "double $E2$" versus $E4$ excitation of the 4+ state if we assume the $E4$ transition is enhanced to five single-particle units. A similar calculation for 45-MeV ^{16}O ions on ^{152}Sm gives a larger ratio of 1500.

As one would expect, the $E4$ excitation is relatively more significant for α particles than for the more highly charged ^{16}O ions. We must also estimate the magnitude of the interference term between "double $E2$" and $E4$ modes of excitation. We have carried out a calculation of the relative size of the interference term for 11-MeV α particles on ^{152}Sm. We find that $(d\sigma_{E4-E2,E2}/d\sigma_{E2,E2})$ at

[20] D. L. Hendrie, N. K. Glendenning, B. G. Harvey, O. N. Jarvis, H. H. Duhm, J. Saudinos, and J. Mahoney, Phys. Letters **26B**, 127 (1968).

TABLE VIII. Coulomb-excitation probabilities from ^{4}He-γ coincidence measurements for ^{152}Sm. (See caption for Table VI.)

J^π	E_i (MeV)	$E_{cut}(J)$ (MeV)	$(P_J)_{expt}$	$(P_J)_{expt}/(P_J)_{theor}$	$R(4/2)_{expt}/R(4/2)_{theor}$
2+	13.0	9.56	4.76×10^{-2}	0.941±0.052	
4+	13.0	9.67	4.89×10^{-4}	1.041±0.057	1.106±0.064

160° is less than 0.02 for an $E4$ enhancement of five single-particle units. At our present level of experimental accuracy, we can neglect the $E4$ contribution to P_4 for α particles and ^{16}O ions.

A summary of our best experimental values for $B(E2, 4\rightarrow6)$ and $B(E2, 6\rightarrow8)$ is given in Table VII. These values are obtained by the use of the relation

$$B(E2, I\rightarrow J)=C^2(I2J;00)B(E2, 0\rightarrow2)\times[R(J/I)_{expt}/R(J/I)_{theor}]. \quad (9)$$

The quantity $B(E2, 0\rightarrow2)/R(J/I)_{theor}$ is nearly independent of the value taken for $B(E2, 0\rightarrow2)$, so that $B(E2, I\rightarrow J)$ is not sensitive to the value taken for $B(E2, 0\rightarrow2)$. Furthermore, the quantity $R(J/I)_{expt}$ depends only on the relative efficiency of the γ-ray detector. Both these features contribute to the accuracy with which the $B(E2, I\rightarrow J)$ can be determined.

Our objective is to compare the experimental ratios of $B(E2)$ values within the rotational band to those expected for a rigid rotor. These comparisons are shown in the last 3 columns of Table VII (the theoretical values for the ratios are given at the bottom of the table). Clearly, the experimental ratios given in columns 4 and 5 depend directly on the values taken for $B(E2, 0\rightarrow2)$. We have used the values given by Stelson and Grodzins and have included the error in $B(E2, 0\rightarrow2)$ in obtaining the error given for the ratio.

A ^{4}He-γ coincident measurement was carried out for ^{152}Sm in order to accurately measure the $B(E2, 2\rightarrow4)$. Table VIII summarizes this experimental result. The $(P_J)_{theor}$ was calculated with the Winther–de Boer program using[18] $B(E2, 0\rightarrow2)$ of 3.40 $e^2\times10^{-48}$ cm^4. From this measurement, we extract the values of (1.94 ± 0.12) $e^2\times10^{-48}$ cm^4 for the $B(E2, 2\rightarrow4)$ for ^{152}Sm.

IV. DISCUSSION AND CONCLUSIONS

Multiple Coulomb excitation was used to measure $B(E2)$ values between higher members of the ground-state rotational band. The $B(E2, 2\rightarrow4)$ and $B(E2, 4\rightarrow6)$ values were determined to accuracies of 6–10%. The $B(E2, 6\rightarrow8)$ values were determined to accuracies of 15–25%. For the poor rotor ^{152}Sm, the results indicate some increase in the $B(E2)$ values over the rigid-rotor predictions for the higher transitions. The results for the four good-rotor nuclei show smaller $B(E2)$ values between higher rotational states than those given by the rigid-rotor however, rather than larger values predicted by centrifugal stretching. It is still instructive to carry out an interpretation in terms of this model to gain insight as to what extent measurements of $B(E2)$ values with the present accuracy are able to test the model.

A stretching parameter α is defined as $\alpha=B/A$, where $E_I=AI(I+1)-BI^2(I+1)^2$. One can obtain α values based on the energies of the 2+ and 4+ states, and these values are given in the final column of Table IX. The parameter α is also related to the $B(E2)$ values as follows:

$$B(E2, I\rightarrow J)=(5/16\pi)C^2(I2J;00)Q^2(I, J), \quad (10)$$

where

$$Q(I, J)=Q_0\{1+\alpha/2[I(I+1)+J(J+1)-6]\} \qquad I\neq J \quad (11)$$

and

$$Q_0=[(16/5)\pi B(E2, 0\rightarrow2)]^{1/2}. \quad (12)$$

A summary of α values based on $B(E2)$ ratios is given in Table IX and in graphical form in Fig. 5. Columns 2, 3, and 4 list the values used for the ratio $R(4/2)$, $R(6/4)$, and $R(8/6)$ of experiment to theory. These ratios are then used to get $B(E2)$'s by the use of formula (9). Columns 5, 6, and 7 list the values obtained for α by the use of the formulas (10), (11), and (12). Column 8 gives a weighted average value for α based on the results in columns 5, 6, and 7.

The α values determined from the $B(E2)$'s illustrate an important leverage effect as one moves up the rotational band. Although the $B(E2, 6\rightarrow8)$ has only a 25% accuracy compared to 7% for the $B(E2, 2\rightarrow4)$, the resultant value of α from the $B(E2, 6\rightarrow8)$ has about half the error of that based on the $B(E2, 2\rightarrow4)$.

The four nuclei ^{172,174,176}Yb and ^{166}Er have $E(4+)/E(2+)$ ratios that deviate by only 1–2% from the rigid-rotor value. For these nuclei, the errors on the α parameters derived from the measured $B(E2)$ ratios are somewhat larger than the predicted magnitudes of α based on the level positions. Hence, a definitive test of the consistency of α values derived from the two types of information is scarcely possible. However, the unexpected result is that the α values derived from $B(E2)$ ratios are negative. For three nuclei, the observed departures from the rigid-rotor values are somewhat larger than the experimental errors.

The $B(E2)$ measurements for the poor-rotor ^{152}Sm, which has an $E(4+)/E(2+)$ ratio differing from the

rigid-rotor value by 10%, yields a positive value for the α parameter. However, it magnitude is only about half as large as the value obtained from the level positions.

The above conclusions about $B(E2)$ ratios assumed that our ability to interpret the multiple Coulomb-excitation process is not subject to error. Actually, the experimental results reflect the combined influence of $B(E2)$ values and possible inaccuracies in our theoretical treatment of the Coulomb-excitation process. The Winther–de Boer computer program uses the semiclassical theory of Coulomb excitation, which means $\eta = Z_1 Z_2 e^2/\hbar v \rightarrow \infty$. Our experimental conditions resulted in η values of about 50–60 for ^{16}O ions and about 15 for α particles.

An important question is the relation of the magnitudes of the quantal corrections to the semiclassical treatment of multiple Coulomb excitation. We know that in the first-order theory the semiclassical treatment gives quite accurate results for the total and differential cross sections of inelastically scattered particles, provided the characteristic parameters of the excitation process are properly symmetrized. The quantal corrections for higher-order Coulomb-excitation processes have received only limited theoretical investigation. The multiple Coulomb-excitation mechanism that produces the static-quadrupole-moment effect has been studied.[21,22] It was found that quantal corrections to the semiclassical treatment vary as $1/\eta$.

Although quantal corrections for the process that excites the 4+ state by multiple Coulomb excitation (the double-$E2$ mechanism from second-order perturbation treatment) have not yet received theoretical investigation, it is anticipated that these corrections will also vary as $1/\eta$. Our $B(E2, 2\rightarrow 4)$ values from the semiclassical interpretation of α scattering agree well

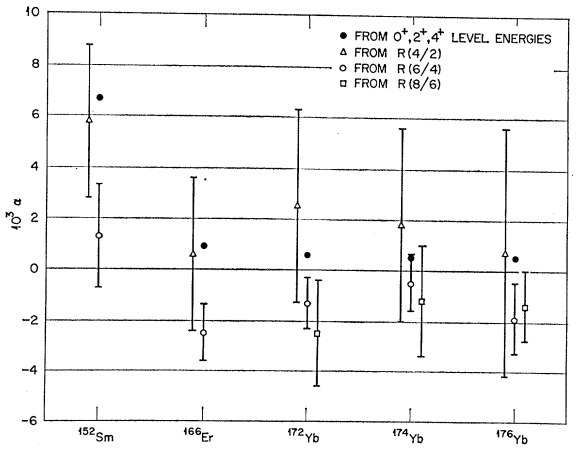

FIG. 5. Comparison of α parameters obtained from several measured $B(E2)$ ratios and from 2+ and 4+ level energies.

[21] U. Smilansky, Nucl. Phys. **A112**, 185 (1968).
[22] K. Alder and H. K. A. Pauli, Nucl. Phys. **A128**, 193 (1969).

TABLE IX. Summary of α parameters obtained from measured $B(E2)$ ratios and from level positions. Errors in $B(E2; 0\rightarrow 2)$ have been included in the values given in columns 2, 3, and 4.

Nucleus	Expt/Theor $R(4/2)$	Expt/Theor $R(6/4)$[a]	$R(8/6)$[a]	$10^3\,\alpha_{4/2}$	$10^3\,\alpha_{6/4}$	$10^3\,\alpha_{8/6}$	$10^3\,\langle\alpha\rangle$	$(10^3\,B/A)$[b]
^{152}Sm	1.120±0.063[c]	1.072±0.113	...	5.8±3.0	1.3±2.0	...	2.7±1.7	6.7±1.1
^{166}Er	1.012±0.060[d]	0.865±0.057	...	0.6±3.0	−(2.5±1.1)	...	−(2.1±1.0)	0.9±0.2
^{172}Yb	1.050±0.077[e]	0.930±0.055	0.75±0.19	2.5±3.8	−(1.3±1.0)	−(2.5±2.1)	−(1.3±0.9)	0.6±0.1
^{174}Yb	1.036±0.077[e]	0.970±0.065	0.87±0.21	1.8±3.8	−(0.5±1.1)	−(1.2±2.2)	−(0.5±1.0)	0.5±0.1
^{176}Yb	1.015±0.098[e]	0.899±0.071	0.85±0.14	0.7±4.9	−(1.9±1.4)	−(1.4±1.4)	−(1.6±1.0)	0.5±0.1

[a] Average values taken from Table VI.
[b] Calculated from the 0+, 2+, and 4+ level energies.
[c] Average of the results in Table III and Table VIII.
[d] An average of half-life measurements by A. C. Li and A. Schwarzschild, Phys. Rev. **129**, 2664 (1963), and by H. W. Kugel, E. G. Funk, and J. W. Mihelich, Phys. Rev. **165**, 1352 (1968).
[e] From $B(E2; 4\rightarrow 2)/B(E2; 2\rightarrow 0)$ in Table III.

with $B(E2, 2\rightarrow4)$ values for similar nuclei obtained from lifetime measurements (and the rigid-rotor prediction). Since these $B(E2)$ values seem to be correct to within a few percent, we would expect that, from a $1/\eta$ variation, quantal corrections for ^{16}O excitation of the 4+ state are no larger than 1 or 2%. Of course, quantal corrections for excitation of the 6+ and 8+ states should be larger. However, our method of interpretation, which examines a ratio such as $P(6+)/P(4+)$, should eliminate a common portion of the quantal correction. In conclusion, we suspect it is unlikely that the observed departures of $B(E2)$ values from the rigid-rotor values are attributable to quantal corrections to the Coulomb-excitation process. There is, however, a distinct need for theoretical studies of quantal corrections to multiple Coulomb excitation.

To what extent can the present results on $B(E2)$ values be compared to other similar results? We have already mentioned that, to within the experimental errors, the $B(E2, 2\rightarrow4)$ values for the good rotors agree with the rigid-rotor prediction. Lifetime measurements of similar 4+ states have produced $B(E2, 2\rightarrow4)$ values of comparable accuracy and have also been in agreement with the rigid-rotor value.

The recent results from Berkeley on lifetimes measured by the "plunger" method make a particularly useful comparison with the present results. Diamond *et al.*[23] found the following values for ^{152}Sm:

$$B(E2, 2\rightarrow4) = (1.87\pm0.05)\times10^{-48}\ e^2\ \text{cm}^4$$

and

$$B(E2, 4\rightarrow6) = (1.75\pm0.09)\times10^{-48}\ e^2\ \text{cm}^4.$$

These values compare very well with our values of

$$B(E2, 2\rightarrow4) = (1.94\pm0.12)\times10^{-48}\ e^2\ \text{cm}^4$$

and

$$B(E2, 4\rightarrow6) = (1.66\pm0.17)\times10^{-48}\ e^2\ \text{cm}^4.$$

Diamond *et al.*[24] have also used the plunger method to measure the lifetimes of collective transitions in the nuclei ^{156,158,160}Er. These nuclei are not very good rotors; the best is ^{160}Er, which has an $E(4+)/E(2+)$ ratio of 3.1. It is quite interesting that the $B(E2)$ values obtained for this rather poor rotor show no increase over the rigid-rotor values as one moves up the spin sequence. In fact, the $B(E2)$ values are smaller than the rigid-rotor values with assigned errors that barely overlap the rigid-rotor values. These lifetime results for ^{160}Er suggest the same trend in $B(E2)$ behavior as those we have established from multiple Coulomb excitation for the four good-rotor nuclei.

[23] R. M. Diamond, F. S. Stephens, R. Nordhagen, and K. Nakai, Proceedings of the of the International Conference on Properties of Nuclear States, Montreal, 1969 (unpublished), paper No. 2.7.

[24] R. M. Diamond, F. S. Stephens, W. H. Kelly, and D. Ward, Phys. Rev. Letters **22**, 546 (1969).

PHYSICAL REVIEW C VOLUME 1, NUMBER 4 APRIL 1970

Analysis of the ^{208}Pb$(d, p)^{209}$Pb g.s. Reaction

K. KING AND BRUCE H. J. MCKELLAR
Department of Theoretical Physics, University of Sydney, Sydney, New South Wales, Australia
(Received 16 October 1969)

The ^{208}Pb$(d, p)^{209}$Pb ground-state reaction is analyzed using the method of Butler, Hewitt, McKellar, and May. Using proton parameters fitted to elastic scattering data and Rosen's neutron parameters, good agreement with the proton angular distribution is obtained when the energy of the incident deuteron is above the Coulomb barrier. The spectroscopic factor extracted from the data is 0.65±0.1.

I. INTRODUCTION

As an alternative to the distorted-wave Born-approximation (DWBA) approach to the theory of stripping reactions, Butler, Hewitt, McKellar, and May (BHMM)[1] proposed a method in which the cross section for the reaction (assuming spinless deuterons, neutrons, and protons) is written as

$$d\sigma/d\Omega = [S/(1-S)^2]\,|\,M_S\,|^2, \qquad (1)$$

where S is the spectroscopic factor. The matrix element M_S can be calculated from the optical potentials for the neutron and proton. The optical potential for the deuteron is not required. For generalization of Eq. (1) to the real world, in which particles have spins, we refer the reader to BHMM.

In the present paper, we discuss the application of Eq. (1) to the deuteron-stripping reaction on ^{208}Pb, which leads to the $2g_{9/2}$ ground state of ^{209}Pb. Experimental angular distributions for this reaction are available at several energies both above and below the Coulomb barrier, thus providing a useful test of the BHMM theory.

The neutron optical potential was not determined directly by optical-model analysis because there is a lack of sufficient neutron elastic-scattering data for the isotope ^{208}Pb. Our results show, however, that stripping calculations based on a combination of Rosen's neutron potential[2] and a proton potential that fits (p, p)

[1] S. T. Butler, R. G. L. Hewitt, B. H. J. McKellar, and R. M. May, Ann. Phys. (N.Y.) **43**, 282 (1967).

[2] L. Rosen, J. G. Beery, A. S. Goldhaber, and E. H. Auerbach, Ann. Phys. (N.Y.) **34**, 96 (1965).